

## Article

# Strength and Microstructural Evolution of Magnesium Phosphate Cement Mortar in Plateau Environment

Zhiping Ren <sup>1</sup>, Jihui Qin <sup>2,\*</sup> , Zhiyang Gao <sup>3</sup>, Pengyu Huang <sup>4</sup>, Yaning Kong <sup>1,4</sup> and Xiaowei Gu <sup>5</sup>

<sup>1</sup> School of Civil Engineering, Chongqing University, Chongqing 400045, China; 20155665@cqu.edu.cn (Z.R.); kongyaning1224@126.com (Y.K.)

<sup>2</sup> Department of Civil, Architectural, and Environmental Engineering, Missouri University of Science and Technology, Rolla, MO 65401, USA

<sup>3</sup> Changjiang River Scientific Research Institute of Changjiang Water Resources Commission, Wuhan 430010, China; gaozy@mail.crsri.cn

<sup>4</sup> China West Construction Academy of Building Materials, Chengdu 610000, China; 13290060802@163.com

<sup>5</sup> School of Resource and Civil Engineering, Northeastern University, Shenyang 110819, China; guxiaowei@mail.neu.edu.cn

\* Correspondence: jqin@mst.edu

**Abstract:** Climatic conditions in plateau areas can enormously affect the properties and microstructure of cement-based materials. This research investigates the strength development and microstructural changes in magnesium phosphate cement (MPC) mortars in a plateau environment. Experiments were conducted in parallel in a plateau area (Lhasa) and a plain area (Chengdu) to evaluate the effects of the water-to-binder ratio ( $w/b = 0.12, 0.14$  and  $0.16$ ) and sand-to-binder ratio ( $s/b = 0.5, 0.75$  and  $1$ ) on the compressive and flexural strength of MPC mortars. At the same time, hydration products were characterized via XRD, TGA, and SEM/EDX micro-analyses, and the porosity of the materials was also analyzed via MIP. The results demonstrated that curing in a plateau environment resulted in a decrease in workability and yielded higher strength at an early age (before 1 day) but degraded the long-term (180-day) strength of MPC mortars when compared with curing in a plain environment, irrespective of  $w/b$  and  $s/b$  ratios. Unlike the plain group, the plateau group revealed the deterioration of microstructures over time, including the decrease in struvite content, the morphology change in struvite crystals, and the increase in porosity, which resulted in the degradation of mechanical properties between 1 and 180 days. The strength loss can be effectively alleviated at lower  $w/b$  and  $s/b$  ratios.

**Keywords:** magnesium phosphate cement; plateau environment; strength loss; struvite; porosity



**Citation:** Ren, Z.; Qin, J.; Gao, Z.; Huang, P.; Kong, Y.; Gu, X. Strength and Microstructural Evolution of Magnesium Phosphate Cement Mortar in Plateau Environment. *Buildings* **2024**, *14*, 410. <https://doi.org/10.3390/buildings14020410>

Academic Editor: Binsheng (Ben) Zhang

Received: 13 December 2023

Revised: 28 January 2024

Accepted: 31 January 2024

Published: 2 February 2024



**Copyright:** © 2024 by the authors. Licensee MDPI, Basel, Switzerland. This article is an open access article distributed under the terms and conditions of the Creative Commons Attribution (CC BY) license (<https://creativecommons.org/licenses/by/4.0/>).

## 1. Introduction

With the growing demand for infrastructure construction in plateau areas, like Tibet in China and Karbi Anglong in India, cement concrete is widely used in buildings, pavements, bridges, dams, runways, etc. [1,2]. Compared with plain areas, the climatic environments in plateau areas are much harsher, characterized by low atmospheric pressure, dry air, strong solar radiation, low temperatures, a large daily temperature difference, and low precipitation [3–5]. The severe environment in plateau regions leads to more serious deterioration and damage in concrete structures than in plain regions [5]. Therefore, a large number of existing concrete structures in plateau areas face an urgent need for repair and strengthening. In damaged areas of highways, bridge decks, and airfields, it is often desirable for maintenance engineers to carry out repair work with the least disruption possible to transportation. However, in the plateau area with low or sub-zero temperatures, it may take quite a long time for conventional repair materials to harden to a sufficient strength, making it difficult to meet the requirements for the rapid repair of concrete [6]. Therefore, there is a clear need to develop new repair materials for the rapid repair of concrete structures in plateau areas.

Magnesium phosphate cement (MPC), also known as chemically bonded magnesium phosphate ceramic [7], has been receiving a growing amount of attention over recent decades as an alternative to traditional Portland cement (PC), and is being actively studied for special applications, such as construction and rapid repairs [8–10], hazardous waste or nuclear waste solidification [10,11], and biomedical materials [12]. The microstructure and performance development of MPC rely on the acid–base neutralization reaction between MgO and phosphate to yield struvite,  $\text{MgNH}_4\text{PO}_4 \cdot 6\text{H}_2\text{O}$  (Equation (1)) or K-struvite,  $\text{MgKPO}_4 \cdot 6\text{H}_2\text{O}$  (Equation (2)) [7,13–15]. Due to the unique compositions and reaction mechanisms, MPC has many advantageous characteristics compared with traditional PC and other inorganic binders. These include rapid setting, high early and later strength, good volume stability, excellent bonding properties with old concrete, high resistance to steel corrosion, good wear resistance, and salt corrosion resistance [7,16–19].



More recently, several studies [9,20–22] have shown that MPC can provide the essential requirements for the rapid repair of concrete in cold environments. The laboratory and field investigation by Jia [9,22] revealed that light-burned MgO-modified MPC concrete can set rapidly and reach a 2 h compressive strength of more than 30 MPa at  $-20^\circ\text{C}$ . In terms of durability, an MPC paste containing limestone and silica fume exhibited a minimum strength residual ratio of more than 85% after 400 freeze–thaw cycles in water, sodium chloride solution, or sodium sulfate solution [21]. Ji [22] reported that MPC mortar can acquire good resistance to sulfate freeze–thaw at an early age (1 day). These results demonstrate that MPC can be promising for the emergency repair of concrete in severe cold environments. Nevertheless, the conditions of negative temperatures and freezing and thawing cannot totally reflect the extreme environmental characteristics of plateau areas. More knowledge concerning the properties of MPC in plateau areas is required prior to its practical application.

The impacts of the plateau environment on the performance of MPC have not been previously reported. Instead, there have been extensive experimental studies for PC-based materials in this respect. Drying and low-air-pressure conditions in the plateau area can accelerate the moisture evaporation of cement paste and affect its hydration reaction, which results in a loose and porous microstructure and the deterioration of pore structures [1,23]. Under low air pressure, the nucleation and development of air bubbles become harder, which results in an abnormal air-void structure and causes the workability and compressive strength of concrete to deteriorate [3,4]. Furthermore, low air pressure could aggravate drying shrinkage in cement mortar [2] and cause a deterioration in the durability of concrete in terms of water variation and water absorption, permeability, and deicer salt scaling [5,24]. Meanwhile, frost-heaving stress can be generated in concrete under low temperatures, causing damage to its structure and leading to a decrease in long-term strength [4,25]. In brief, the plateau environment will have adverse impacts on the microstructure, mechanical properties, and durability of PC-based materials. Considering that MPC materials have distinctly different reaction mechanisms and phase compositions from PC-based materials, the climatic environments in plateau areas may have different effects on their properties and microstructure.

The purpose of this study is to investigate the fresh properties, mechanical properties, and microstructural behaviors of MPC materials when they are kept in a plateau environment. The setting time, workability, and compressive and flexural strength of MPC mortars prepared with different water-to-binder (w/b) and sand-to-binder (b/s) ratios were comparatively studied in a high-altitude plateau area and a low-altitude plain area. The microstructural evolution was also studied via X-ray diffraction (XRD), thermogravimetric analysis (TGA), mercury intrusion porosimetry (MIP), and scanning electron microscopy coupled with energy dispersive X-ray spectroscopy (SEM/EDX). The experimental findings

are anticipated to provide solid support for the application of MPC-based materials in plateau environments.

## 2. Materials and Methods

### 2.1. Raw Materials

Dead-burned magnesia (MgO) powder was purchased from Tiansheng Magnesium Industry, Liaoning, China, and was produced via the calcination of magnesite at 1700 °C for 6 h, followed by crushing and grinding. The main chemical composition and particle size distribution of the dead-burned MgO are shown in Table 1 and Figure 1, respectively. Industrial grade ammonium dihydrogen phosphate (ADP,  $\text{NH}_4\text{H}_2\text{PO}_4$ ) with a purity of 99% was employed. Sodium tetraborate decahydrate (Borax,  $\text{Na}_2\text{B}_4\text{O}_7 \cdot 10\text{H}_2\text{O}$ ) with a purity of 99% was selected as a setting retarder. ADP and borax were ground separately and passed through a 0.15 mm sieve prior to use. Quartz sand was used as the fine aggregate; it had a fineness modulus of 2.9, a water absorption of 0.51%, an apparent density of 2580 kg/m<sup>3</sup>, and a bulk density of 1580 kg/m<sup>3</sup>.

**Table 1.** Chemical composition of the dead-burned magnesia (wt.%).

Oxides	MgO	CaO	SiO <sub>2</sub>	Fe <sub>2</sub> O <sub>3</sub>	Al <sub>2</sub> O <sub>3</sub>	Others	L.O.I.
Content	90.80	1.37	2.87	1.29	2.40	1.03	0.24

Note: L.O.I. is the loss on ignition.

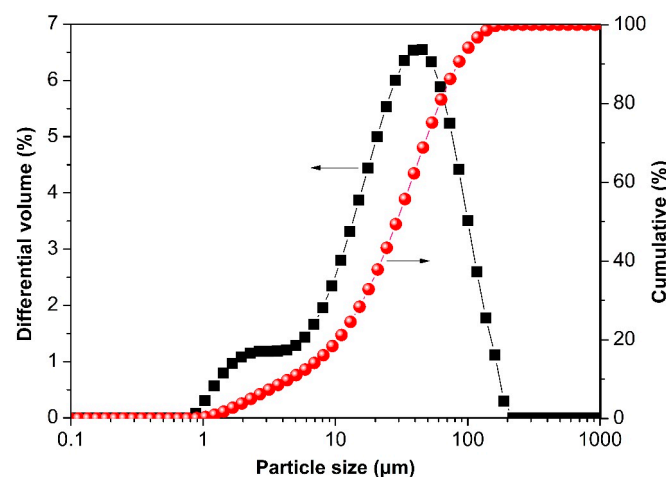


**Figure 1.** Differential and cumulative volumes versus the particle size distribution of the dead-burned magnesia.

### 2.2. Mix Proportion

The mix proportions of the investigated MPC mortars are shown in Table 2. The MPC binder consisted of magnesia, ADP, and borax. The mass ratio of magnesia-to-ADP (M/P) was fixed at 4:1, and the addition level of borax was 5%, by the total mass of magnesia and ADP. As shown in Table 2, five mortar formulations were designed to compare and investigate the effects of w/b and s/b ratios on the mechanical properties and microstructure of MPC mortar in plateau and plain environments. Based on a fixed s/b ratio of 0.75, the w/b ratio was adjusted to 0.12, 0.14, and 0.16 to prepare S0.75W0.12, S0.75W0.14, and S0.75W0.16 samples, respectively. At a constant w/b ratio of 0.14, the s/b ratios of 0.50, 0.75, and 1.00 were employed to fabricate S0.5W0.12, S0.75W0.14, and S1.0W0.14 samples, respectively.

**Table 2.** Mix proportion of MPC mortars.

Samples	Binder Components			M/P	s/b	w/b
	Magnesia	ADP	Borax			
S0.75W0.12	1	0.25	0.062	4	0.75	0.12
S0.75W0.14	1	0.25	0.062	4	0.75	0.14
S0.75W0.16	1	0.25	0.062	4	0.75	0.16
S0.5W0.14	1	0.25	0.062	4	0.50	0.14
S1.0W0.14	1	0.25	0.062	4	1.00	0.14

### 2.3. Specimen Preparation and Curing

MPC mortars were prepared according to the mix designs presented in Table 2. For the mixing procedure, all dry components, including magnesia, ADP, borax, and quartz sand, were firstly stirred for 60 s at a low speed, and then water was added and mixed for 90 s at a low speed, followed by another 90 s of stirring at a high speed until the mixtures were homogenized. After that, the fresh MPC mortar was poured into steel molds with dimensions of 40 mm × 40 mm × 160 mm and vibrated for 60 s to ensure the compaction of mixtures. Paste specimens with formulations corresponding to the MPC mortars with various w/b ratios, as listed in Table 2, were prepared in the same manner as the mortar specimens and used for XRD and TGA analyses. They are referred to as P-W0.12, P-W0.14, and P-W0.16. Both paste and mortar specimens were demolded after 1 h of adding water and subsequently cured in a laboratory environment until testing.

In this study, specimen preparation and curing were performed in parallel in two laboratory environments at two test sites, namely at Lhasa on the Qinghai–Tibet Plateau with a high altitude of 3650 m and at Chengdu on the Chengdu Plain with a low altitude of 500 m. Figure 2 shows the variations in three key parameters in the laboratory environments during the whole curing period, including the average temperatures, relative humidities, and atmospheric pressures. These parameters were recorded via synchronization using a Comet D4141 thermo-hygro-barometer (Czech). It is shown that, compared with the plain environment, the plateau environment has the climatic characteristics of low atmospheric pressure, dry air, and low temperature. The harsh climate of the plateau area may pose a great challenge to performance and microstructure development in MPC materials.

### 2.4. Test Methods

#### 2.4.1. Setting Time and Workability Measurement

Setting time of MPC mortar was determined using a Wuxi Jianyi SN-100 digital mortar setting time tester (Wuxi, China) according to Chinese Standard JC/T 2537-2019 [26]. When MPC mortar started to set, the setting time measurements were made every 30 s. Since the interval between the initial setting time and final setting time of MPC mortar was very short, only the initial setting time was recorded as the setting time. The workability of fresh MPC mortar was evaluated using the mini-slump cone and flow table as per the guidelines described in [27]. The mortar was allowed to flow until no changes in the flow diameter were observed. Each mix was repeated. It should be noted that setting time and workability measurements were performed in both plain and plateau environments with an identical temperature of 20 °C.

#### 2.4.2. Mechanical Strength Tests

For flexural strength testing, following the Chinese standard GB/T 17671-2021 [28], prisms of 40 mm × 40 mm × 160 mm were tested using a Wuxi Jianyi TYE-300D testing machine (Wuxi, China) with a loading rate of 0.05 kN/s and a span of 100 mm at 3 h, 1 day, and 180 days. For each batch, the flexural strength was the average of three specimens. Six fractured halves after flexural strength testing were used for the measurement of compressive strength. In the compression test, the specimens with a contact area of 40 mm × 40 mm were tested using a TYE-300D testing machine (China) with a loading rate

of 2.4 kN/s. Averages of six samples for each mixture were reported as the compressive strength test results.

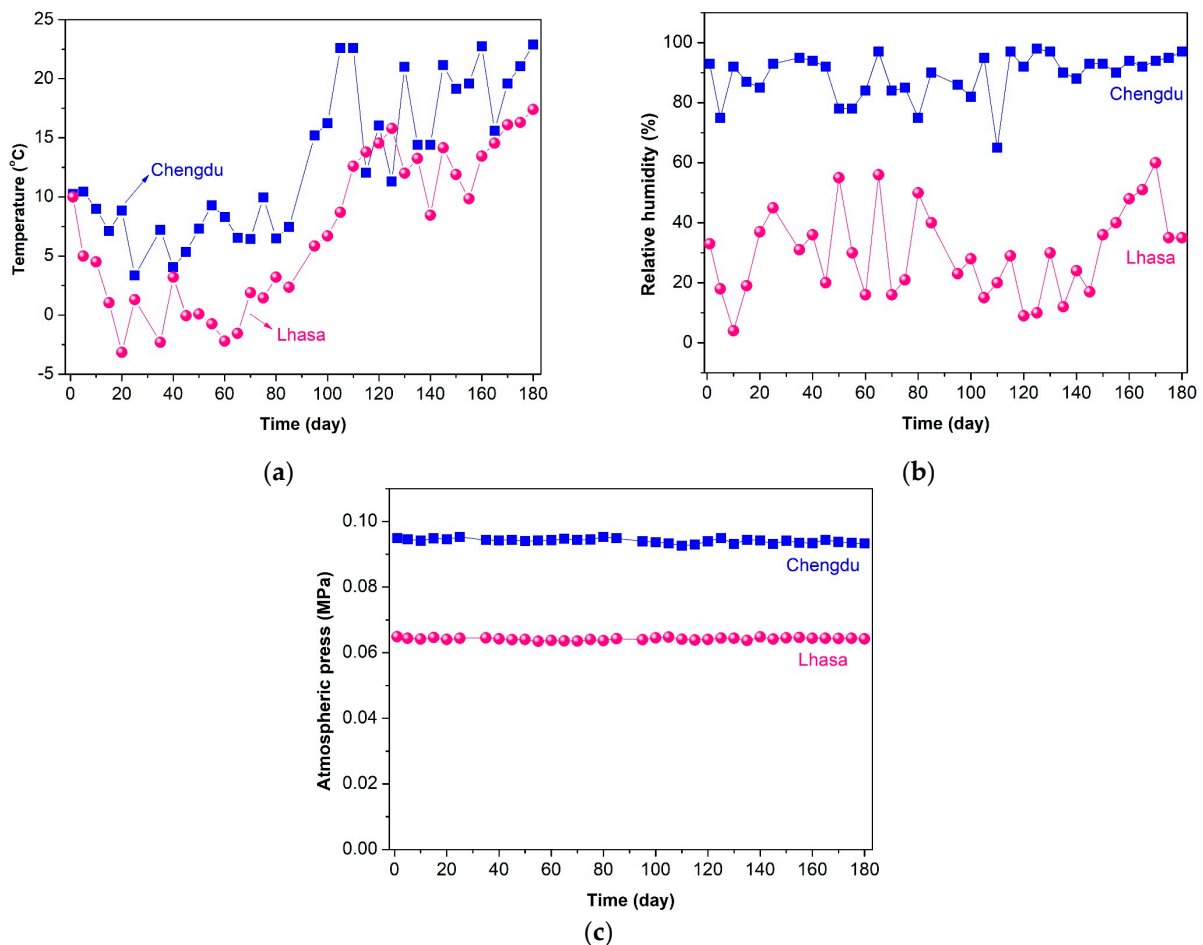


**Figure 2.** Three key parameters of the laboratory environment in a plain area, Chengdu and a plateau area, Lhasa: (a) average temperature; (b) relative humidity; and (c) atmospheric pressure.

#### 2.4.3. X-ray Diffraction (XRD) Analysis

At specific hydration ages, paste specimens were crushed into small pieces and soaked in absolute ethanol for 24 h to stop hydration. After that, they were dried in the oven at 40 °C for another 24 h to remove residual organic solvents, and then stored in a sealed bottle. The samples were further ground by hand to fine powders with a particle size below 75  $\mu\text{m}$  prior to XRD analysis. XRD patterns were collected using a Bruker-AXS D8 Discover X-ray diffractometer (Karlsruhe, Germany) equipped with a Lynxeye detector (Cu  $K\alpha$ , 1.54184 Å). The X-ray generator was set at 40 mA and 40 kV. The continuous scanning mode was 3 °/min, and the  $2\theta$ -range was 5–85°.

#### 2.4.4. Thermogravimetric Analysis (TGA)

Thermogravimetry (TG) and differential scanning calorimetry (DSC) data were collected using a PerkinElmer Diamond TG analyzer (Waltham, MA, USA). Around 10 mg of ground MPC powders were placed in an alumina ceramic crucible. The sample was heated from room temperature to 1000 °C at a heating rate of 10 °C/min and under nitrogen atmosphere with a nitrogen flow of 50 mL/min.

#### 2.4.5. Pore Structure Analysis

After compression strength tests, intact blocks were collected from the broken specimens and further fractured into small particles with sizes of 2–5 mm. Fractured samples

were soaked in absolute ethanol for 48 h and then placed in a drying oven at 40 °C for 48 h. To obtain information on the pore structures of MPC mortars at specific ages, MIP tests were performed on fractured samples by using a Micromeritics' Autopore IV 9500 (Norcross, GA, USA). The test pressures were in the range of 0.518 to 32,923.57 psi, corresponding to the pore size range of 348.63  $\mu\text{m}$  to 5.5 nm.

#### 2.4.6. SEM Observation

The microstructure of MPC mortars was observed using an FEI Inspect F50 scanning electron microscope (Hillsboro, OR, USA) with an accelerating voltage of 10 kV and a current of 10 nA, coupled with EDAX super octane equipment. Before the SEM tests, the dried samples were sprayed with gold in a vacuum environment.

### 3. Results and Discussion

#### 3.1. Setting Time and Workability

Table 3 shows the setting times and flow diameters of the MPC mortars determined in plain and plateau environments. As shown in Table 3, there were negligible differences between the setting times of MPC mortars determined in plain and plateau areas. Considering that the setting time tests were conducted at the same temperature, it is inferred that the low relative humidity and atmospheric pressure did not show a significant impact on the initial setting reaction of MPC. However, the flow diameters of MPC mortars in the plateau area were obviously lower than those obtained in the plain area. Similar observations have been reported in PC-based mixtures [4]. This could be explained by the reduced air content of mixtures due to the low air pressure in the plateau area. It is also found that the increase in the w/b ratio from 0.12 to 0.16 did not significantly change the setting time but substantially improved the workability, as expected. The MPC mortar with a low s/b ratio exhibited an acceptable setting time and excellent flowability. A higher proportion of sand slightly shortened the setting time and significantly decreased the flowability, tending to cause difficulties in placement and compaction.

**Table 3.** Setting times and flow diameters of MPC mortars determined in plain and plateau areas.

Samples	Setting Time (min)		Flow Diameter (mm)	
	Plain	Plateau	Plain	Plateau
S0.75W0.12	18.0	17.0	180	165
S0.75W0.14	18.0	18.5	240	215
S0.75W0.16	18.5	18.0	270	240
S0.5W0.14	20.0	19.0	260	240
S1.0W0.14	15.0	14.5	195	170

#### 3.2. Compressive and Flexural Strength

Figure 3 depicts the compressive strength development in the MPC mortar in the climatic environments of plain and plateau areas. All samples had a 3 h compressive strength over 20 MPa and a 1-day strength over 40 MPa, highlighting the rapid strength gains for the MPC mortar in both plain and plateau environments. For the plain group, the compressive strength increased with the curing age, irrespective of the w/b and s/b ratios. At the earliest age of 3 h, the compressive strength appeared to decrease very slightly with an increase in the w/b ratio from 0.12 to 0.16. However, after further aging, a substantial decrease in the strength at the higher w/b ratio became apparent. At the given w/b ratio of 0.14, the increase in the s/b ratio from 0.5 to 1.0 did not significantly lower both the early age and long-term compressive strength. The strength development trend in MPC mortar in the plain environment is consistent with those reported in the previous literature [18,29].

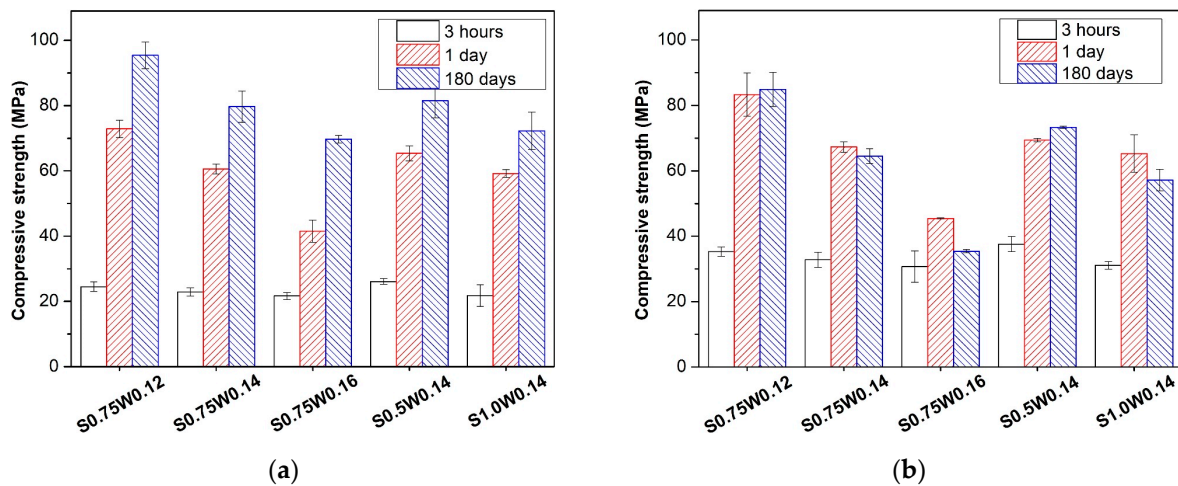


**Figure 3.** Compressive strength development in the MPC mortars in different climatic environments: (a) plain area and (b) plateau area.

As for the plateau group, similar downward trends in compressive strength were observed at higher  $w/b$  and  $b/s$  ratios. It is interesting to point out that the plateau group exhibited higher early age (3 h and 1-day) compressive strength than the plain one, while negligible increases or even reductions in the compressive strength were observed between 1 and 180 days. In the plateau condition, compared with the 1-day compressive strength, the 180-day compressive strength of S0.75W0.12, S0.75W0.14, and S0.75W0.16 varied by 1.92%,  $-4.16\%$ , and  $-22.03\%$ , respectively. In other words, the larger the  $w/b$  ratio, the greater the compressive strength loss. At the age of 180 days, the compressive strength of S0.5W0.14, S0.75W0.14, and S1.0W0.14 varied by 5.62%,  $-4.16\%$ , and  $-12.40\%$ , respectively, compared with those at the age of 1 day in the plateau environment. Similarly, a higher  $s/b$  ratio led to a greater compressive strength loss between 1 and 180 days. The strength loss could be mainly related to the decreased degree of hydration and the increased amount of macropores in MPC mortar after a long period of aging in drying and low-air-pressure conditions, which is discussed further in the following sections.

The flexural strength development in the MPC mortars in plain and plateau environments is shown in Figure 4. Similar to Figure 3, the MPC mortars showed rapid flexural strength gain at an early age due to the fast acid–base reaction between MgO and ADP and the resulting rapid formation of binding phase (mainly struvite). The plain group still gained 30–70% strength increases between 1 and 180 days, whereas slight strength losses of 10–20% occurred for the plateau group over the same period, except for S0.75W0.12 with a relatively low  $w/b$  ratio. Obviously, the increases in  $w/b$  and  $s/b$  ratios led to lower flexural strength in both the plain and plateau environments. Compared with the plain group, the increases in  $w/b$  and  $s/b$  ratios resulted in more significant flexural strength losses for the plateau group, particularly at a later age.

To better compare the strength development in the MPC mortars in plain and plateau environments, the strength increase rates of the plateau group with respect to the plain one are provided in Table 4. It is obvious that both compressive and flexural strength increase rates were positive at an early age (3 h and 1 day) for each MPC mortar mix, but turned negative with long-term age (180 days). As for the compressive strength, its increase rate at 3 h was more than 40%, suggesting that the plateau condition is conducive to early compressive strength gain. At the age of 180 days, the increase in the  $w/b$  ratio from 0.12 to 0.16 increased the compressive and flexural strength loss rates from 11.0% to 49.2% and from 2.5% to 32.7%, respectively. Additionally, the increase in the  $s/b$  ratio from 0.5 to 1.0 also resulted in a higher rate of strength loss. The above results indicate that the MPC materials with relatively low water and sand contents can effectively withstand the adverse effects of the harsh plateau environment on their long-term strength development.

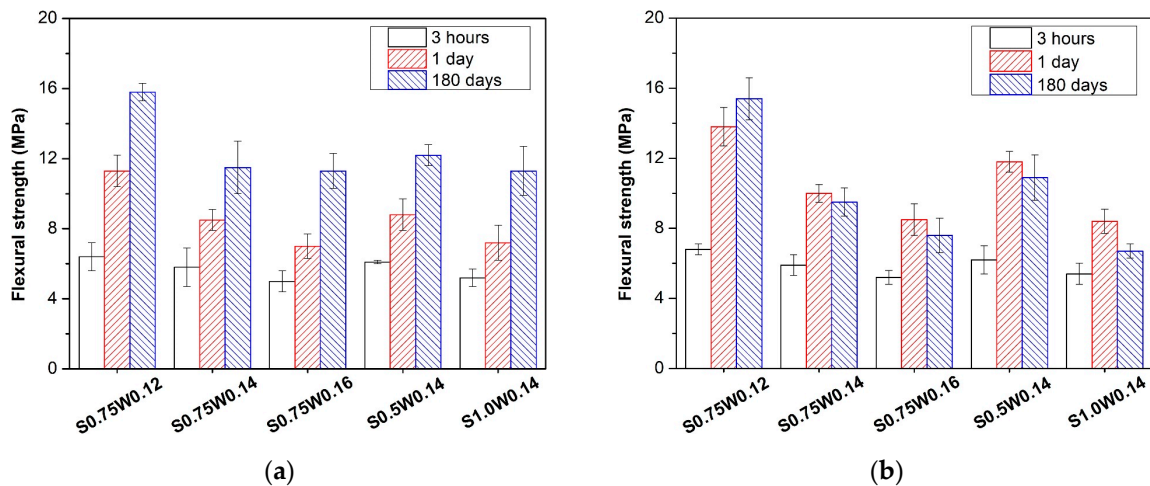


**Figure 4.** Flexural strength development in the MPC mortar in different climatic environments: (a) plain area and (b) plateau area.

**Table 4.** Strength increase rates of the plateau group with respect to the plain group (%).

Sample	Compressive Strength Increase Rate			Flexural Strength Increase Rate		
	3 h	1 Day	180 Days	3 h	1 Day	180 Days
S0.75W0.12	44.1	14.3	−11.0	6.2	22.1	−2.5
S0.75W0.14	43.2	11.1	−19.1	1.7	17.6	−17.4
S0.75W0.16	41.5	9.4	−49.2	4.0	21.4	−32.7
S0.5W0.14	44.1	6.1	−10.1	1.6	34.1	−10.7
S1.0W0.14	42.7	10.3	−20.9	3.8	16.7	−40.7

Note: the strength increase rate ( $K_{si}$ ) was defined as  $K_{si} = (R_{plateau} - R_{plain})/R_{plain}$ , where  $R_{plain}$  and  $R_{plateau}$  are the strengths of the MPC mortars prepared in the plain and plateau areas, respectively.

### 3.3. Hydration Products

The XRD patterns of the MPC paste samples (i.e., P-W0.12, P-W0.14, and P-W0.16) in plain and plateau environments are shown in Figure 5. Struvite ( $MgNH_4PO_4 \cdot 6H_2O$ ) was found to be the main crystalline hydration product forming in both plain and plateau environments, which can provide a cementing ability for MPC materials [16,30]. Apart from struvite, no other crystalline products were observable in the patterns. A large amount of periclase ( $MgO$ ) was still identified in all cases, as magnesia was added in excess (M/P mass ratio of 4:1). The phase assemblage of MPC pastes did not appear to change with varying climatic environments. However, the relative intensity of the main struvite reflection at  $2\theta = 20.8^\circ$  of the plain group appeared to be slightly higher than that of the plateau one, especially at 180 days, which may suggest the slightly lower degree of crystallinity of struvite in the plateau environment.

The semi-quantitative analysis of unreacted  $MgO$  and generated struvite was conducted using Jade 6.5 software, and the results are shown in Table 5. As can be seen from Table 5, whether in a plain or plateau environment, with the increase in the w/b ratio from 0.12 to 0.16, the unreacted  $MgO$  content decreased commensurately with an increased struvite content, which suggests that a higher water content (w/b ratio) can lead to an increased yield of struvite and thus improve the hydration degree of MPC. Compared with the plain group, the  $MgO$  or struvite content of the plateau group was almost unchanged at 1 day. However, at the age of 180 days, the plateau group revealed a slightly higher  $MgO$  content and lower struvite content, indicating a lower hydration degree in comparison to the plain one.

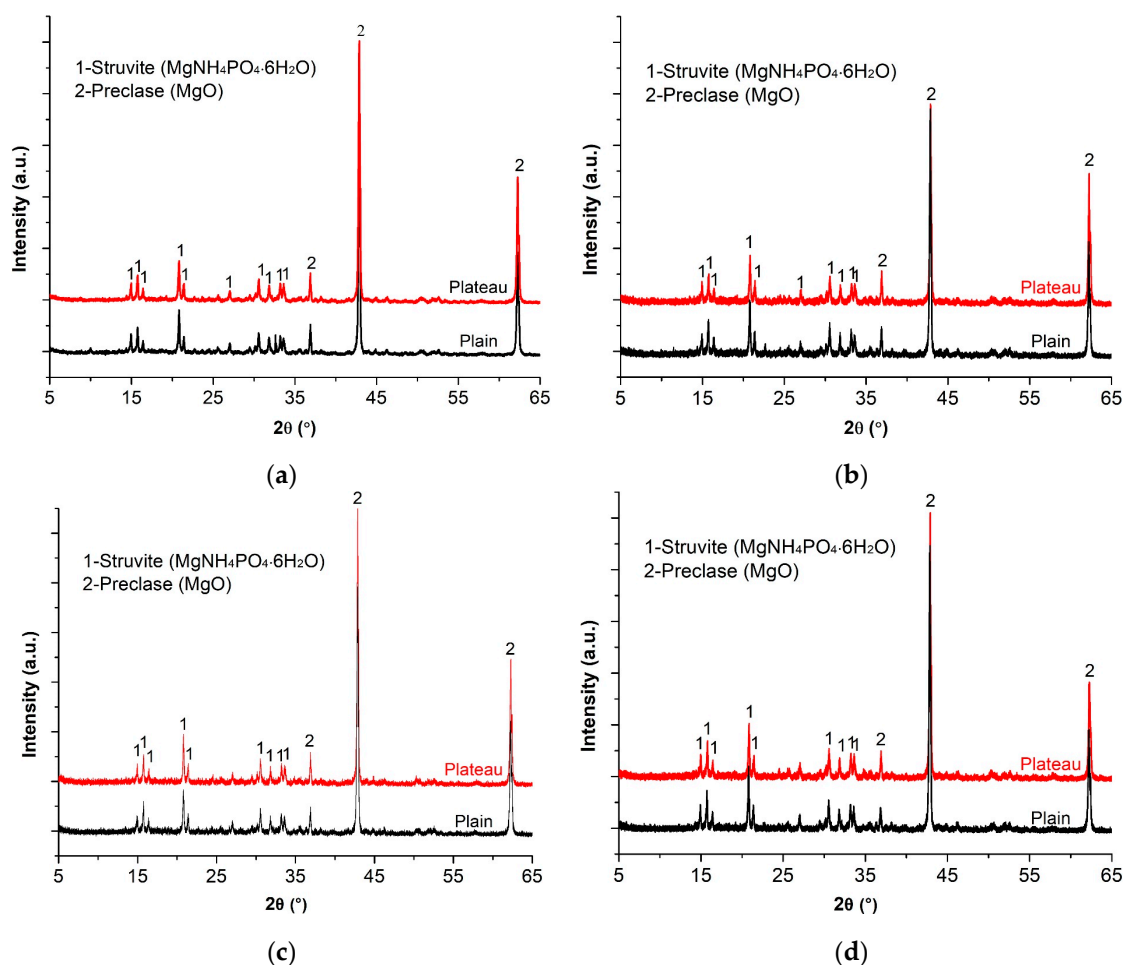


**Figure 5.** XRD patterns of various MPC paste samples cured in the climatic environments of plain and plateau regions: (a) P-W0.14 at 1 day; (b) P-W0.12 at 180 days; (c) P-W0.14 at 180 days; (d) P-W0.16 at 180 days.

**Table 5.** Relative contents of MgO and struvite in MPC paste samples cured in plain and plateau environments.

Samples	Curing Age (Day)	Curing Condition	MgO (wt.%)	MgNH <sub>4</sub> PO <sub>4</sub> ·6H <sub>2</sub> O (wt.%)
P-W0.14	1	Plain	92.5	7.5
		Plateau	92.7	7.3
P-W0.12	180	Plain	92.5	7.5
		Plateau	93.1	6.9
P-W0.14	180	Plain	90.3	9.7
		Plateau	91.2	8.8
P-W0.16	180	Plain	89.8	10.2
		Plateau	90.3	9.7

Figure 6 shows the TG-DSC curves of the MPC paste samples in plateau and plain environments. The TG-DSC curves of MPC pastes in both plateau and plain environments had roughly the same shapes, irrespective of w/b ratios and curing ages. For all the MPC pastes, a sharp endothermic peak occurred at a temperature of around 100 °C, which is mainly attributed to the dehydration of struvite (MgNH<sub>4</sub>PO<sub>4</sub>·6H<sub>2</sub>O) to dittmarite (MgNH<sub>4</sub>PO<sub>4</sub>·H<sub>2</sub>O) [30]. The broad endotherm at ~220 °C is due to the decomposition of dittmarite to MgHPO<sub>4</sub> [31]. The weight loss observed between 50 and 300 °C is closely

linked to the amount of hydration product. At the early age of 1 day, curing in the plateau environment slightly reduced the content of hydration product struvite compared with curing in the plain environment. In the plain group, the mass losses in the temperature range of 50–300 °C were 18.1%, 18.4%, and 19.1% for P-W0.12, P-W0.14, and P-W0.16 at the age of 180 days, respectively. As for the plateau group, the mass losses observed up to 300 °C were 17.1%, 17.4%, and 18.2% for P-W0.12, P-W0.14, and P-W0.16, respectively. These results indicate that the increase in the  $w/b$  ratio from 0.12 to 0.16 slightly increased the quantity of struvite and the plateau group had a slightly smaller quantity of struvite compared with the plain one. This is consistent with the XRD analysis, as shown in Figure 5 and Table 5. Generally, the lower the atmospheric pressure, the greater the moisture evaporation, which leads to a lower amount of available water for continuous hydration. This results in lower formation of struvite in the low-air-pressure environment than in the normal-pressure environment. Meanwhile, MPC is sensitive to drying conditions, and even drying at low temperature or in a partial vacuum can slightly damage K-struvite [32]. Thus, the low temperature and air pressure and dry climate conditions in the plateau environment may adversely affect the stability of struvite and reduce the struvite content, which is harmful to the long-term strength.

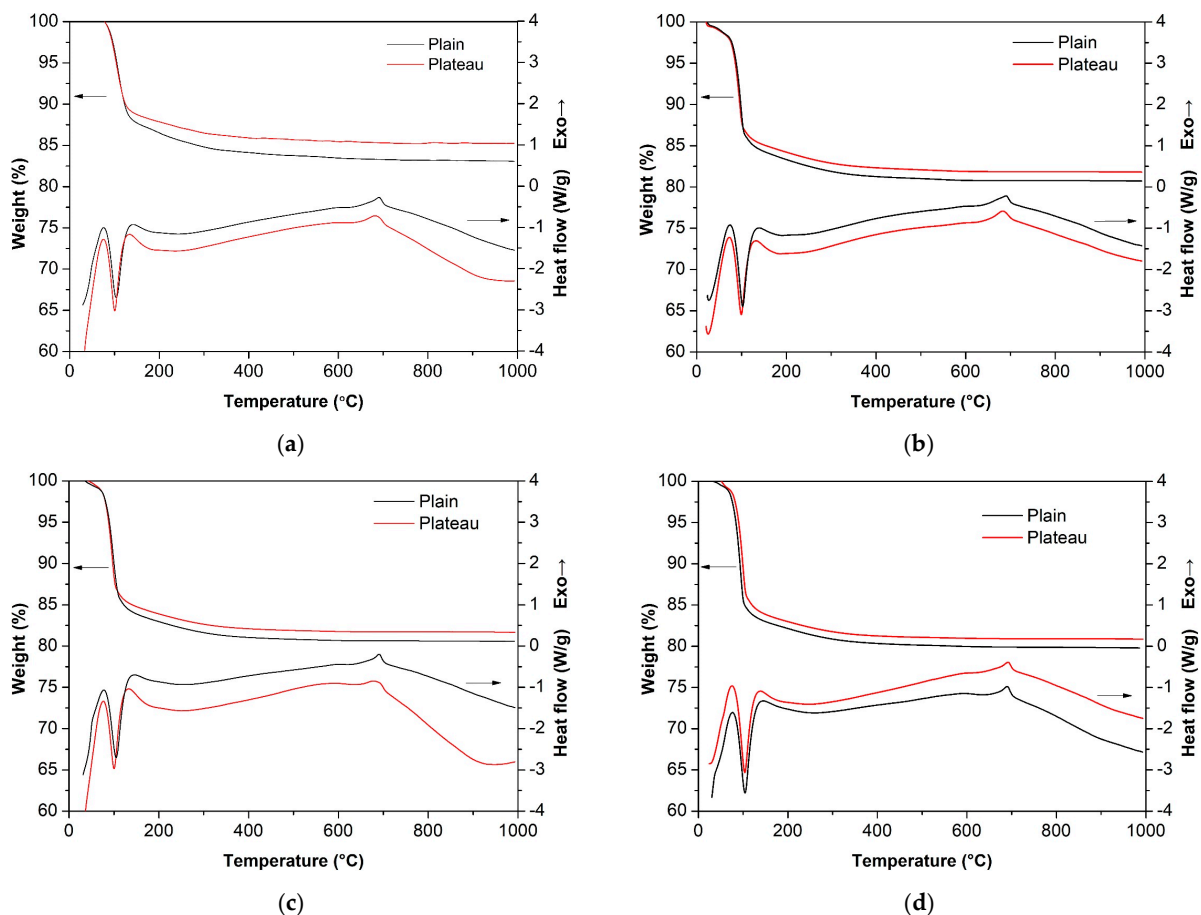


**Figure 6.** TG-DSC curves of various MPC paste samples cured in climatic environments of plain and plateau regions: (a) P-W0.12 at 1 day; (b) P-W0.12 at 180 days; (c) P-W0.14 at 180 days; (d) P-W0.16 at 180 days.

### 3.4. Pore Structure

Figure 7 and Table 6 show the pore size distribution and total porosity of M0.75W0.14 after 1 day of curing in plain and plateau environments. In cementitious materials, the pores can be typically classified into four categories based on the pore sizes: gel pores (<10 nm), transitional pores (10–100 nm), capillary pores (100 nm–1  $\mu$ m), and macropores

(>1  $\mu\text{m}$ ) [33]. M0.75W0.14 mortars cured in plateau and plain environments presented similar bimodal pore size distributions (between 10 nm and 4000 nm diameter) and had roughly the same total porosities of 21.34% and 21.31%, respectively. However, the MPC mortar cured in the plateau environment had a lower volume of macropores or air voids, in comparison to that cured in the plain environment. A significant portion of air voids in the MPC mortar came from air and ammonia gas bubbles entrained in the fresh mixture. Research has shown that the stability of bubbles in fresh concrete at low atmospheric pressure becomes worse than at normal air pressure [3,34], which may explain why MPC mortar in the plateau environment had a lower number of macropores than in the plain environment at the early stage. This observation could explain the higher early strength in the plateau group.

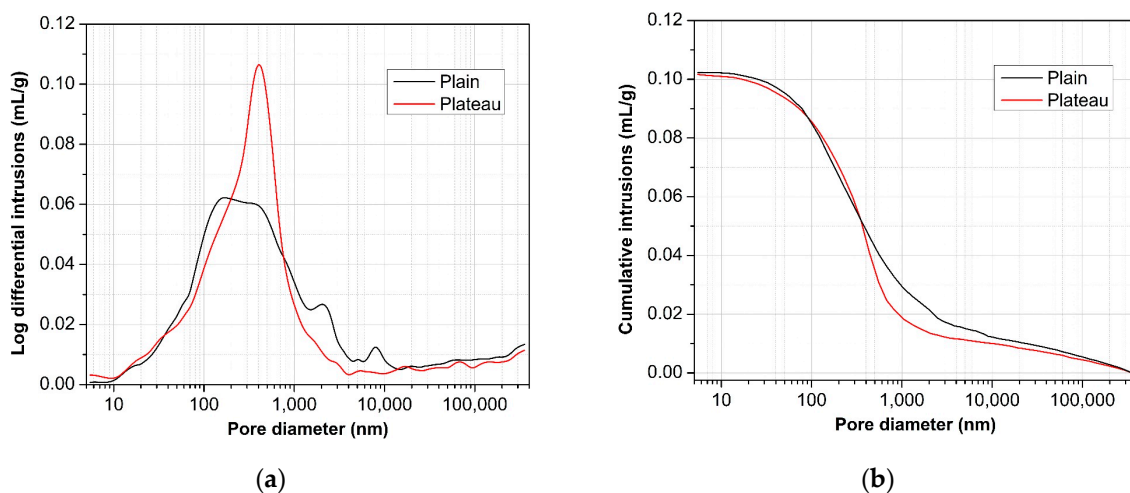


**Figure 7.** MIP analysis of M0.75W0.14 after 1 day of curing in plain and plateau conditions: (a) log differential intrusions; (b) cumulative intrusions.

**Table 6.** Total porosities and pore size distributions in the MPC mortar samples.

Sample	Curing Age (Day)	Curing Condition	Total Porosity (%)	Pore Size Distribution (%)			
				Gel Pores (<10 nm)	Transitional Pores (10–100 nm)	Capillary Pores (100 nm–1 $\mu\text{m}$ )	Macropores (>1 $\mu\text{m}$ )
S0.75W0.14	1	Plain	21.34	0.06	3.60	11.70	5.98
		Plateau	21.31	0.16	3.23	14.09	3.83
S0.75W0.12	180	Plain	14.49	0.11	2.04	7.72	4.62
		Plateau	14.69	0.36	2.26	8.84	3.23
S0.75W0.14	180	Plain	16.37	0.10	2.16	10.81	3.30
		Plateau	19.39	0.03	2.59	10.25	6.52
S0.75W0.16	180	Plain	16.47	0.25	2.71	8.90	4.61
		Plateau	21.95	0.38	3.52	10.97	7.08

The pore size distribution and total porosity of MPC mortars after 180 days of curing in the plain and plateau environment are shown in Figure 8 and Table 6. Bimodal distributions were still observed for all the 180-day-old samples. Generally, a smaller most-probable pore size was measured for the plateau group in comparison to the plain one. For M0.75W0.14 in the plain environment, increasing the curing age from 1 day to 180 days led to a reduction of 4.97% in the total porosity. As mentioned in the previous literature [15], the continuous reaction between MgO and phosphate can reduce both capillary pores and macropores. However, a substantial increase in the volume of macropores was measured for M0.75W0.14 in the plateau environment between 1 and 180 days, which could explain the strength degradation shown in Figures 3b and 4b. Compared with the plain group, the cumulative

mercury entry curve of the plateau group shifted toward the right and upward, indicating that curing in the plateau environment increases the threshold pore size and total porosity of MPC mortar. For instance, the total porosity of M0.75W0.16 in the plateau environment was 21.95%, much higher than the total porosity (16.47%) of the sample in the plain environment. Overall, the larger the  $w/b$  ratio, the greater the increase in porosity in the mortar in the plateau environment. A higher  $w/b$  ratio caused increases in the volume of capillaries and air pores, owing to more free water being included in the MPC mortars. Reducing the  $w/b$  ratio could effectively reduce the negative impact of the plateau environment on the pore structure of MPC mortar in the later stage.

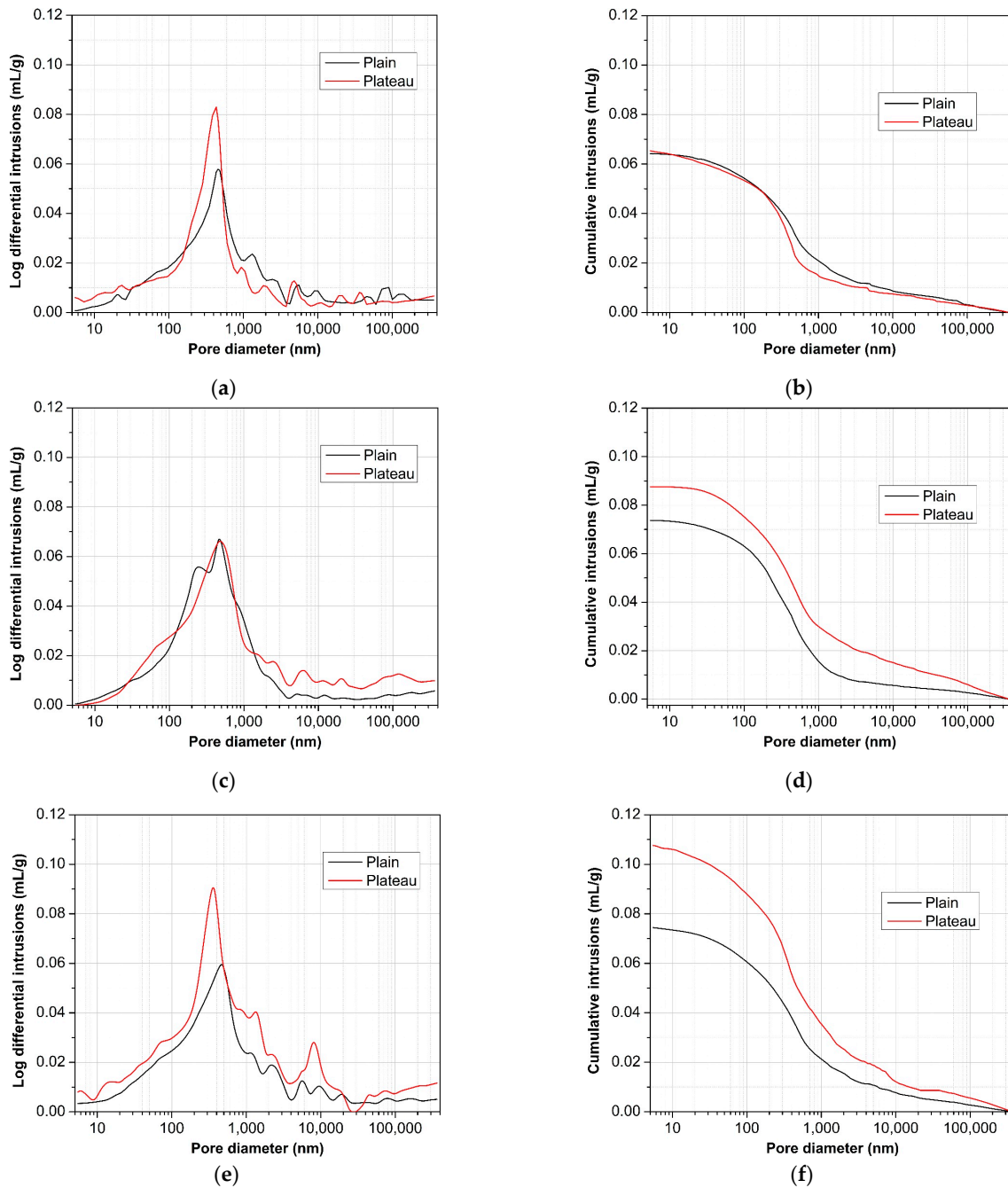


**Figure 8.** Pore size distributions in the MPC mortar samples after 180 days of curing in the climatic environments of plain and plateau regions: (a,b) S0.75W0.12; (c,d) S0.75W0.14; and (e,f) S0.75W0.16.

### 3.5. Microstructure

Figure 9 shows the typical morphologies of the crystals presented in M0.75W0.14 after 180 days of curing in plain and plateau environments. The EDX analysis from these crystals is shown in Table 7. As shown in Figure 9a, plenty of magnesia particles were not completely consumed by the chemical reactions and wrapped with the reaction products, and act as a hard skeleton in the binding matrix. In the plain mortar (Figure 9b), closely aggregated large tabular crystals were formed and can be assigned to struvite according to the EDX analyses. Compared with the plain sample, less regular crystals of a smaller size were formed in the plateau samples (Figure 9c). Microcracks and voids were present throughout these crystals, constructing a looser microstructure than that in the plain sample. This agrees well with the porosity results in Figure 8 and Table 6. In addition, some needle-like crystals were observed in the plateau samples (Figure 9d). By combing the EDX analysis and published observations [32], it can be inferred that these were struvite needles. For the MPC mortar cured in the plateau environment, the climatic conditions of low temperature, low pressure, and drying would facilitate the rearrangement of the internal particles of the massive and plate-like leading morphology of struvite, causing it to change into a rod- or needle-like crystal, which is not conducive to the bonding between hydration products, resulting in an increase in porosity and thus a strength loss.

**Table 7.** Elemental composition of crystals observed within M0.75W0.14 after 180 days of curing in plain and plateau environments.

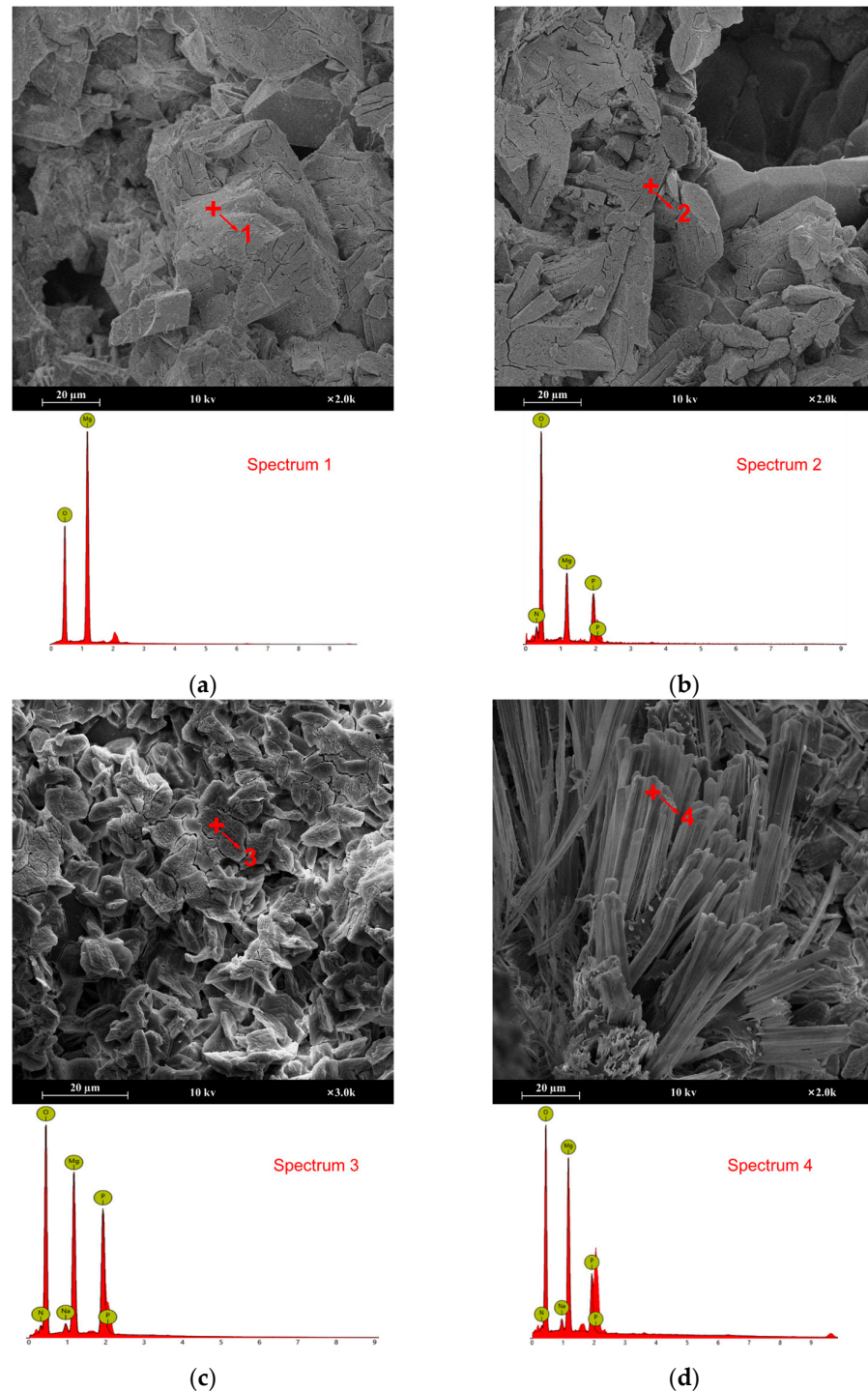
Spectrum	Chemical Element (Atomic, %)				
	O	Mg	P	N	Na
1	56.82	43.18	/	/	/
2	67.25	11.76	11.22	9.76	/
3	63.63	16.30	11.22	7.64	1.21
4	64.59	21.06	6.58	5.88	1.89

Figure 10 shows the SEM morphologies of the interface between cement paste and sand in MPC mortars after 180 days of curing in plain and plateau environments. All samples showed distinct boundaries between sand and matrix. For the plain group (Figure 10a–c), the hydration products were closely combined with the sand particles. M0.75W0.12 displayed a fairly compact matrix and interface owing to the low w/b ratio. The increase in w/b ratio yielded a less compact matrix and interfacial zone, which can be induced by water films as a result of local excess water [16,35]. As for the plateau group (Figure 10d–f), more noticeable microcracks were observed in the cement paste, as well as in the interfacial zone. This could be due to the accelerated moisture evaporation and dehydration of cement paste under drying and low-air-pressure conditions.

### 3.6. Further Discussion

The MPC mortars cured in the plateau environment gained higher early strength than those cured in the plain environment; even the struvite content of the former was slightly lower, and their porosities were basically the same. This strength increase could be related to the poor stability of air or ammonium gas bubbles during very early age in a low air pressure condition, which can reduce the volume of large pores or air voids and thus diminish the negative impact of large pores on strength development. However, the mechanical properties of the MPC mortar in the plateau environment degraded at a later age when compared with those in the plain environment. This is mainly ascribed to the lower hydration degree and more porous microstructure of the MPC during aging in the severe plateau environment. On the one hand, the low air pressure and drying conditions can accelerate the evaporation of free water in the specimens [1] and may negatively affect the stability of crystal water in struvite [31], which not only prevents the further hydration of cement but also increases the volume of capillaries and large pores and the

total porosity. On the other hand, the low-temperature condition delays the hydration process, leading to a lower degree of hydration [36]. Moreover, when curing in the plateau environment, the morphologies of struvite crystals were observed to change from large blocks or tabular plates into rod-/needle-like crystals (Figure 9), which will affect the mutual bonding between hydration products and, in turn, cause strength loss.



**Figure 9.** Typical SEM morphologies and EDS analysis of the crystals: (a) unreacted MgO particles and (b) closely aggregated tabular struvite in M0.75W0.14 after 180 days of curing in the plain environment; (c) struvite with an irregular shape; and (d) needle-like crystals in M0.75W0.14 after 180 days of curing in the plateau environment.

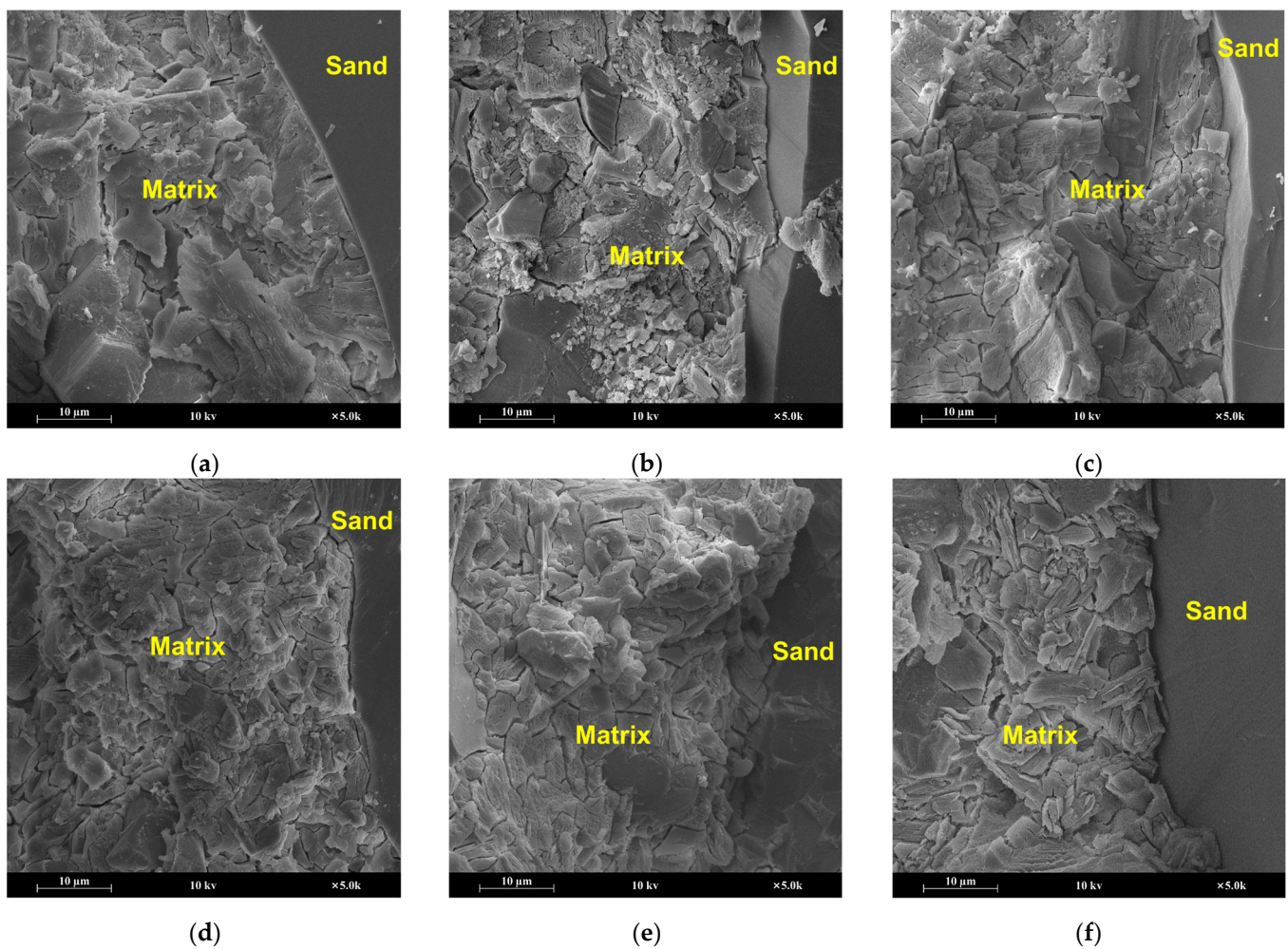


**Figure 10.** Typical SEM morphologies of the interface between matrix and sand in MPC mortars: (a) M0.75W0.12, (b) M0.75W0.14, and (c) M0.75W0.16 after 180 days of curing in plain environment; and (d) M0.75W0.12, (e) M0.75W0.14, and (f) M0.75W0.16 after 180 days of curing in plateau environment.

The w/b ratio is a key parameter in the mix design of MPC materials and the optimization of their microstructure and properties. Theoretically, for an MPC with a molar M/P ratio  $> 1$ , the optimal w/b ratio must satisfy Equations (1) or (2) so that both water and phosphate can be completely converted into struvite or k-struvite [13,37]. In this study, the optimal amount of water for MPC with a mass M/P ratio of 4 is calculated as  $\sim 0.13$ . For M0.75W0.12, a w/b ratio of 0.12 is slightly less than that required for complete reaction, meaning that the amount of water can be exhausted through the continuous formation of the hydration product struvite and no available water will be left to generate additional capillary and large pores in either the plain or plateau environment. Thus, negligible differences in the volume of capillaries and large pores and the total porosity between the plain and plateau samples were observed. Due to the depletion of water, the expansion crystal pressure caused by water freeze–thaw is negligible and has less adverse impacts on the compressive and flexural strength of M0.75W0.12 in the plateau environment. As the w/b ratio increases, excess water in the slurry is segregated in pores within the volume and evaporates gradually during aging to form more harmful capillaries and large pores, especially in the plateau environment. This has more negative effects on the mechanical properties and frost resistance durability of the matrix.

#### 4. Conclusions

In this paper, the fresh properties and strength development in the MPC mortars in plain and plateau environments were comparatively studied, and the similarities and differences in their microstructures, such as hydration products, pore structures, and microscopic morphologies, in plain and plateau environments were comprehensively analyzed, leading to the following conclusions.

(1) The MPC mortar cured in the plateau environment had lower flowability and higher early age (3 h and 1-day) strength but lower long-term (180-day) strength when compared with that cured in the plain environment, irrespective of  $w/b$  and  $s/b$  ratios. Moreover, curing in the plateau environment can degrade the long-term strength of MPC mortars.

(2) At the early stage, the struvite content of the MPC pastes in the plateau environment was slightly lower than in the plain environment. However, the MPC mortars in the plateau environment had basically the same porosity as those in plain environment and had a lower volume of harmful macropores, which could be responsible for the higher early age strength in the plateau environment.

(3) Compared with the MPC mortars cured in the plain environment, the MPC mortars cured in the plateau environment revealed a low struvite content, higher porosity (especially the volume of capillaries and large pores) and more micro-cracks within the binding matrix at the later age. In addition, curing in the plateau environment favored the formation of rod-/needle-like struvite crystals instead of large blocks or tabular crystals, which could reduce the cohesion between the hydration products. The deterioration of microstructures over time led to the degradation of the mechanical properties.

(4) This study reveals the important roles of  $w/c$  and  $s/b$  ratios on the strength and microstructure development in MPC mortars in a plateau environment. Reducing  $w/b$  and  $s/b$  ratios can effectively alleviate the deteriorations in mortar performance in the plateau environment. It is worth noting that the strength reductions caused by microstructure degradation disappear when the  $w/b$  ratio used is lower than that required for complete reaction.

The experimental findings demonstrate that the optimized MPC can obtain a good workability and robust early age and long-term strength. However, there are other properties besides workability and mechanical strength that are required for MPC to be suitable for rapid and durable repair in plateau areas. These include, but are not limited to, the bond property, volume stability, and durability. Experimental investigations into some of these properties are in progress, and the results will be presented in another paper.

**Author Contributions:** Conceptualization, J.Q., Y.K. and X.G.; methodology, Z.R. and Y.K.; formal analysis, Z.R., J.Q. and Y.K.; investigation, Z.R., Z.G. and P.H.; data curation, Z.R. and P.H.; writing—original draft, Z.R. and Z.G.; writing—review and editing, J.Q. and X.G.; supervision, J.Q.; project administration, J.Q. and Y.K.; funding acquisition, Y.K. All authors have read and agreed to the published version of the manuscript.

**Funding:** This research was funded by the National Natural Science Foundation of China (Grant No. 52234004) and the CRSRI Open Research Program (Program SN: CKMV2021878/KY).

**Data Availability Statement:** The data were generated during the experimental study and are contained within the article.

**Conflicts of Interest:** The authors declare no conflicts of interest.

#### References

1. Huo, J.; Wang, Z.; Zhang, T.; Ji, X.; Zhang, H.; He, R. The evolution of early-age cracking of cement paste cured in low air pressure environment. *J. Build. Eng.* **2022**, *52*, 104489. [[CrossRef](#)]
2. Wang, H.; Long, G.; Tang, Z.; Xie, Y.; Ma, G.; Tang, C.; Liu, S.; Ren, X. The volume stability of cement-based materials under different extreme environments in the plateau: Experimental evolution. *J. Build. Eng.* **2022**, *62*, 105370. [[CrossRef](#)]
3. Zeng, X.; Lan, X.; Zhu, H.; Long, G.; Xie, Y. Investigation on air-voids structure and compressive strength of concrete at low atmospheric pressure. *Cem. Concr. Compos.* **2021**, *122*, 104139. [[CrossRef](#)]

4. Huo, J.; Wang, Z.; Chen, H.; He, R. Impacts of low atmospheric pressure on properties of cement concrete in plateau areas: A literature review. *Materials* **2019**, *12*, 1384. [[CrossRef](#)] [[PubMed](#)]
5. Ge, X.; Ge, Y.; Li, Q.; Cai, X.; Yang, W.; Du, Y. Effect of low air pressure on the durability of concrete. *Constr. Build. Mater.* **2018**, *187*, 830–838. [[CrossRef](#)]
6. Hu, X.; Peng, G.; Niu, D.; Zhao, N. Effect of early frost environment on service performance of concrete. *J. Build. Mater.* **2020**, *23*, 1061–1070.
7. Wagh, A.S. *Chemically Bonded Phosphate Ceramics*; Elsevier: Amsterdam, The Netherlands, 2004; pp. 264–267.
8. Qiao, F.; Chau, C.K.; Li, Z. Property evaluation of magnesium phosphate cement mortar as patch repair material. *Constr. Build. Mater.* **2010**, *24*, 695–700. [[CrossRef](#)]
9. Jia, X.; Luo, J.; Zhang, W.; Qian, J.; Li, J.; Wang, P.; Tang, M. Preparation and application of self-curing magnesium phosphate cement concrete with high early strength in severe cold environments. *Materials* **2020**, *13*, 5587. [[CrossRef](#)] [[PubMed](#)]
10. Wagh, A.S. Recent Progress in Chemically Bonded Phosphate Ceramics. *ISRN Ceram.* **2013**, *2013*, 983731. [[CrossRef](#)]
11. Gardner, L.J.; Corkhill, C.L.; Walling, S.A.; Vigor, J.E.; Murray, C.A.; Tang, C.C.; Provis, J.L.; Hyatt, N.C. Early age hydration and application of blended magnesium potassium phosphate cements for reduced corrosion of reactive metals. *Cem. Concr. Res.* **2021**, *143*, 106375. [[CrossRef](#)]
12. Yu, L.; Xia, K.; Gong, C.; Chen, J.; Dai, H. An injectable bioactive magnesium phosphate cement incorporating carboxymethyl chitosan for bone regeneration. *Int. J. Biol. Macromol.* **2020**, *160*, 101–111. [[CrossRef](#)]
13. Qin, J.; Qian, J.; Dai, X.; You, C.; Ma, H.; Li, Z. Effect of water content on microstructure and properties of magnesium potassium phosphate cement pastes with different magnesia-to-phosphate ratios. *J. Am. Ceram. Soc.* **2021**, *104*, 2799–2819. [[CrossRef](#)]
14. Xu, B.; Lothenbach, B.; Leemann, A.; Winnfeld, F. Reaction mechanism of magnesium potassium phosphate cement with high magnesium-to-phosphate ratio. *Cem. Concr. Res.* **2018**, *108*, 140–151. [[CrossRef](#)]
15. Zhang, G.; Wang, Q.; Li, Y.; Zhang, M. Microstructure and micromechanical properties of magnesium phosphate cement. *Cem. Concr. Res.* **2023**, *172*, 107227. [[CrossRef](#)]
16. Qin, J.; Dai, F.; Ma, H.; Dai, X.; Li, Z.; Jia, X.; Qian, J. Development and characterization of magnesium phosphate cement based ultra-high performance concrete. *Compos. Part B Eng.* **2022**, *234*, 109694. [[CrossRef](#)]
17. Tang, H.; Qian, J.; Qin, J.; Li, Z.; Jia, X.; Yue, Y.; Dai, F. Electrochemical behavior of steel bars in magnesium phosphate cement. *Cem. Concr. Res.* **2023**, *169*, 107167. [[CrossRef](#)]
18. Qin, J.; Qian, J.; You, C.; Fan, Y.; Li, Z.; Wang, H. Bond behavior and interfacial micro-characteristics of magnesium phosphate cement onto old concrete substrate. *Constr. Build. Mater.* **2018**, *167*, 166–176. [[CrossRef](#)]
19. Li, Y.; Shi, T.; Li, J. Effects of fly ash and quartz sand on water-resistance and salt-resistance of magnesium phosphate cement. *Constr. Build. Mater.* **2016**, *105*, 384–390. [[CrossRef](#)]
20. Jia, X.; Li, J.; Wang, P.; Qian, J.; Tang, M. Preparation and mechanical properties of magnesium phosphate cement for rapid construction repair in ice and snow. *Constr. Build. Mater.* **2019**, *229*, 116927. [[CrossRef](#)]
21. Chong, L.; Yang, J.; Xu, Z.; Xu, X. Freezing and thawing resistance of MKPC paste under different corrosion solutions. *Constr. Build. Mater.* **2019**, *212*, 663–674. [[CrossRef](#)]
22. Ji, R.-J.; Li, T.; Yang, J.-M.; Xu, J. Sulfate freeze–thaw resistance of magnesium potassium phosphate cement mortar according to hydration age. *Materials* **2022**, *15*, 4192. [[CrossRef](#)] [[PubMed](#)]
23. Lan, X.; Zeng, X.; Zhu, H.; Long, G. Experimental investigation on fractal characteristics of pores in air-entrained concrete at low atmospheric pressure. *Cem. Concr. Compos.* **2022**, *130*, 104509. [[CrossRef](#)]
24. Huo, J.; Wang, Z.; Ji, X.; Zhang, T.; Zhang, H.; Zhou, X.; Guo, H. Chloride resistance of cement-based materials with paraffin emulsion-nano silica sol cured at low air pressure. *Constr. Build. Mater.* **2023**, *398*, 132498. [[CrossRef](#)]
25. Liu, J.; Xin, Z.; Huang, Y.; Jia, Y. Climate suitability assessment on the Qinghai-Tibet Plateau. *Sci. Total Environ.* **2022**, *816*, 151653. [[CrossRef](#)] [[PubMed](#)]
26. *JC/T 2537-2019; Magnesium Phosphate Repairing Mortar*. Ministry of Industry and Information Technology of the People’s Republic of China [MOIIT], China Building Materials Press: Beijing, China, 2019.
27. Oderji, S.Y.; Chen, B.; Ahmad, M.R.; Shah, S.F.A. Fresh and hardened properties of one-part fly ash-based geopolymer binders cured at room temperature: Effect of slag and alkali activators. *J. Clean. Prod.* **2019**, *225*, 1–10. [[CrossRef](#)]
28. *GB/T 17671-2021; Test Method of Cement Mortar Strength (ISO Method)*. National Standardization Management Committee, People’s Republic of China: Beijing, China, 2021. (In Chinese)
29. Lee, K.-H.; Yoon, H.-S.; Yang, K.-H. Tests on magnesium potassium phosphate composite mortars with different water-to-binder ratios and molar ratios of magnesium-to-phosphate. *Constr. Build. Mater.* **2017**, *146*, 303–311. [[CrossRef](#)]
30. Yu, J.; Qian, J.; Wang, F.; Li, Z.; Jia, W. Preparation and properties of a magnesium phosphate cement with dolomite. *Cem. Concr. Res.* **2020**, *138*, 106235. [[CrossRef](#)]
31. Shi, J.; Zhao, J.; Chen, H.; Hou, P.; Kawashima, S.; Qin, J.; Zhou, X.; Qian, J.; Cheng, X. Sulfuric acid-resistance performances of magnesium phosphate cements: Macro-properties, mineralogy and microstructure evolutions. *Cem. Concr. Res.* **2022**, *157*, 106830. [[CrossRef](#)]
32. Lahalle, H.; Patapy, C.; Glid, M.; Renaudin, G.; Cyr, M. Microstructural evolution/durability of magnesium phosphate cement paste over time in neutral and basic environments. *Cem. Concr. Res.* **2019**, *122*, 42–58. [[CrossRef](#)]

33. Li, Y.; Li, J. Capillary tension theory for prediction of early autogenous shrinkage of self-consolidating concrete. *Constr. Build. Mater.* **2014**, *53*, 511–516. [[CrossRef](#)]
34. Li, X.F.; Fu, Z. Effect of low-pressure of environment on air content and bubble stability of concrete. *J. Chin. Ceram. Soc.* **2015**, *43*, 1076–1082.
35. Samal, D.K.; Ray, S. An improved understanding of the influence of  $w/c$  ratio and interfacial transition zone on fracture mechanisms in concrete. *Mag. Concr. Res.* **2023**, *75*, 847–863. [[CrossRef](#)]
36. Chen, D.; Yu, X.; Liu, R.; Li, S.; Zhang, Y. Triaxial mechanical behavior of early age concrete: Experimental and modelling research. *Cem. Concr. Res.* **2019**, *115*, 433–444. [[CrossRef](#)]
37. Ma, H.; Xu, B. Potential to design magnesium potassium phosphate cement paste based on an optimal magnesia-to-phosphate ratio. *Mater. Des.* **2017**, *118*, 81–88. [[CrossRef](#)]

**Disclaimer/Publisher’s Note:** The statements, opinions and data contained in all publications are solely those of the individual author(s) and contributor(s) and not of MDPI and/or the editor(s). MDPI and/or the editor(s) disclaim responsibility for any injury to people or property resulting from any ideas, methods, instructions or products referred to in the content.